Electronic supplementary information (ESI)

Novel, highly efficient blue-emitting heteroleptic iridium (III) complexes based on fluorinated 1, 3, 4-oxadiazole: tuning to blue by dithiolate ancillary ligands

Lianqing Chen,[a] Han You, [b] Chuluo Yang,*[a] Dongge Ma*[b] and Jingui Qin*[a]

[a] *Department of Chemistry, Hubei Key Lab on Organic and Polymeric Optoelectronic Materials, Wuhan University, Wuhan 430072, China. Fax: 86-27-68756757; Tel: 86-27-68756757; E-mail: clyang@whu.edu.cn*
[b] *State Key Laboratory of Polymer Chemistry and Physics, Changchun Institute of Applied Chemistry, Chinese Academy of Sciences, Changchun 130022, China E-mail: mdg1014@ciac.jl.cn*

1. General information

^{1}H NMR spectra were recorded on Varian Mercury VX-300 MHz spectrometer in $CDCl_3$ which were referenced internally using the residual proton solvent resonance relative to $SiMe_4$ ($\delta = 0$). ^{13}C NMR, ^{31}P NMR externally to 85 % H_3PO_4 and ^{19}F NMR externally to HF were obtained on Varian Unity Inova-600 MHz spectrometer in $CDCl_3$. All chemical shifts are quoted in δ (ppm) using the high frequency positive convention and coupling constants in Hz. Infrared spectra were obtained on a Nicolet SX Fourier transform spectrometer. Elemental analysis of carbon, hydrogen, and nitrogen was performed on a Carlorerba-1106 microanalyzer. Mass Spectra (FAB-MS) was determined by VJ-ZAB-3F Mass Spectrometer. UV-Vis absorption spectra were recorded on Shimadzu 160A UV-Vis recording spectrophotometer. PL spectra were performed on Perkin-Elmer LS 55 luminescence spectrophotometer. Solutions of quinine bisulfate (10^{-5} M in 1.0 N H_2SO_4) ($\Phi = 0.546$) were used as a reference. The equation

$$\Phi_s = \Phi_r (\eta_s^2 A_r I_s / \eta_r^2 A_s I_r)$$

was used to calculate the quantum yields, where Φ_s is the quantum yield of the sample, Φ_r is the quantum yield of the reference, η_s is the refractive index of the solvent, A_s and A_r are the absorbance of the sample and the reference at the wavelength of excitation, and I_s and I_r are the integrated areas of emission bands.

All reactions and manipulations were carried out under argon atmosphere. All silica gel column chromatography was performed with use of silica gel (200~300 mesh). Iridium trichloride hydrate and other chemicals were commercially available and used as received unless otherwise stated.

2. Preparation of 1, 3, 4-oxadiazole ligands

General procedure: 4-substituted benzoic acid (20 mmol) was dissolved into 30 ml of polyphosphoric acid (85 %) under argon atmosphere, and then hydrazine hydrate (15 mmol) was slowly added at room temperature. The mixture

was heated at 80 °C for 4 h. After cooling, the solution was poured into ice water and the solution was adjusted to pH 7-8 with 1N sodium bicarbonate solution. A white precipitate was separated out and the crude product was filtered, washed with water several times, and further purified by column chromatography.

2, 5-Diphenyl-1, 3, 4-oxadiazole (**DOX**): white solid, yield: 78 %. Mp = 138~139 °C. ^{1}H NMR (300 MHz, $CDCl_3$) δ: 7.82 (d, *J* = 7.2 Hz, 4H), 7.52 (q, *J* = 6.0 Hz, 4H), 7.35 (q, *J* = 6.6 Hz, 2H). IR (KBr, cm^{-1}): 1611, 1493, 1303, 1256, 1169. MS (EI): *m/e*, 222 (M^+).

2, 5-Bis (4-fluorophenyl)-1, 3, 4-oxadiazole (**FOX**): white solid, yield: 86 %. Mp = 203~204 °C. ^{1}H NMR (300 MHz, $CDCl_3$) δ: 8.14 (d, *J* = 7.8 Hz, 4H), 7.25 (d, *J* = 8.1 Hz, 4H). ^{19}F NMR ($CDCl_3$, to HF) δ: -109.3. IR (KBr, cm^{-1}): 1604, 1495, 1412, 1258, 1098, 846. MS (EI): *m/e*, 258 (M^+).

3. Preparation of Ir (III) complexes

Cyclometalated chloride-bridged dimers: iridium trichloride hydrate (0.352 g, 1.0 mmol), combined with 2.5 equiv of 1, 3, 4-oxadiazole derivatives, was dissolved in a mixture of 2-ethoxyethanol (30 ml) and water (10 ml), and then refluxed for 24 h. The solution was cooled to room temperature, and the resulting precipitate was collected by filtration and washed with water and ethanol. After dried, the crude product was recrystallized from dichloromethane /hexane (1:1, v/v).

Synthesis of mononuclear iridium complexes: the dimer (0.075 mmol), acetylacetone (25 mg, 0.25 mmol) for **1** and **2**, or $NaEt_2dtc$ (55 mg, 0.25 mmol) for **3**, or KEt_2dtp (56 mg, 0.25 mmol) for **4**, and anhydrous sodium carbonate (Na_2CO_3, 1.0 mmol) were dissolved in 2-ethoxyethanol (10 ml). The mixture was refluxed under argon for 15~16 h. After cooling to room temperature, small quantity water was added. The resulting precipitate was collected by filtration and washed with water, ethanol and hexane. After dried in vacuum, the crude product was purified by column chromatography on silica gel with CH_2Cl_2/petroleum ether (1:1~1:3) as eluent.

Bis(2, 5-diphenyl-1, 3, 4-oxadiazolato-N,C^2)iridium(acetylacetonate) [**Ir(DOX)$_2$(acac)**] (**1**): Green powder, yield (based on the dimer): 86 %. ^{1}H NMR ($CDCl_3$, 300 MHz) δ: 8.23 (d, *J* = 6.6 Hz, 4H), 7.56 (d, *J* = 7.2 Hz, 8H), 6.86 (m, 6H), 5.12 (s, 1H), 1.36 (s, 6H). Anal.Calcd for $C_{33}H_{25}O_4N_4Ir$: C, 54.01; H, 3.43; N, 7.64. Found: C, 53.96; H, 3.39; N, 7.68 %. MS (FAB): *m/e*, 734 (M^+).

Bis(2, 5-bis (4-fluorophenyl)-1, 3, 4-oxadiazolato-N,C^2)iridium(acetylacetonate) [**Ir(FOX)$_2$(acac)**] (**2**): Green powder, yield (based on the dimer): 89 %. ^{1}H NMR ($CDCl_3$, 300 MHz) δ: 8.27 (t, *J* = 8.1 Hz, 4H), 7.64 (t, *J* = 6.6 Hz, 2H), 7.27 (t, *J* = 6.9 Hz, 4H), 6.60 (t, *J* = 7.5 Hz, 2H), 6.51 (d, 2H), 5.14 (s, 1H), 1.62 (s, 6H). ^{19}F NMR ($CDCl_3$, to HF) δ: -106.8, -108.1. Anal. Calcd for $C_{33}H_{21}O_4N_4F_4Ir$: C, 49.19; H, 2.63; N, 6.95. Found: C, 49.36; H, 2.58; N, 6.94 %. MS (FAB): *m/e*, 806 (M^+).

Bis(2, 5-bis (4-fluorophenyl)-1, 3, 4-oxadiazolato-N,C^2)iridium(*N,N*'-diethyldithiocarbamate) [**Ir(FOX)$_2$(Et$_2$dtc)**] (**3**): Light green powder, yield (based on the dimer): 88 %. ^{1}H NMR ($CDCl_3$, 300 MHz) δ: 8.27 (t, *J* = 7.5 Hz, 4H), 7.63 (t, *J* = 6.9 Hz, 2H), 7.28 (t, *J* = 6.9 Hz, 4H), 6.66 (t, *J* = 8.7 Hz, 2H), 6.51 (d, *J* = 9.6 Hz, 2H), 3.82 (m, 2H), 3.54 (m, 2H), 1.29 (t, *J* = 7.2 Hz, 6H). ^{13}C NMR ($CDCl_3$, 600 MHz) δ: 175.4, 166.9, 166.3, 162.9, 162.4, 154.2, 129.3, 129.2, 127.3, 121.6, 120.3, 119.7, 117.3, 110.3, 71.9, 66.8, 63.7, 16.7, 16.6. ^{19}F NMR ($CDCl_3$, to HF) δ: -106.5, -107.4. Anal.Calcd for $C_{33}H_{24}O_2N_5S_2F_4Ir$: C, 46.36; H, 2.83; N, 8.19. Found: C, 46.08; H, 2.76; N, 8.16 %. MS (FAB): *m/e*, 855 (M^+).

Bis(2, 5-bis (4-fluorophenyl)-1, 3, 4-oxadiazolato-N,C^2)iridium(*O,O*'-diethyldithiophosphate) [**Ir(FOX)$_2$(Et$_2$dtp)**] (**4**): Light green powder, yield (based on the dimer): 86 %. ^{1}H NMR ($CDCl_3$, 300 MHz) δ: 8.24 (t, *J* = 5.1 Hz, 4H), 7.63 (t, *J* = 8.1 Hz, 2H), 7.28 (t, *J* = 7.2 Hz, 4H), 6.70 (t, *J* = 6.6 Hz, 2H), 6.43 (d, *J* = 7.5 Hz, 2H), 4.45 (m, 2H), 4.20 (m, 2H), 1.35 (t, *J* = 6.6 Hz, 6H). ^{13}C NMR ($CDCl_3$, 600 MHz) δ: 174.1, 164.1, 162.4, 161.6, 157.6, 128.3, 125.8, 120.6, 119.1, 118.8, 115.7, 115.5, 108.4, 108.3, 42.4, 42.1, 11.7, 11.4. ^{31}P NMR ($CDCl_3$, to H_3PO_4) δ: 106.5. ^{19}F NMR ($CDCl_3$, to HF) δ: -105.4, -106.2. Anal.Calcd for $C_{32}H_{24}O_4N_4S_2PF_4Ir$: C, 43.09; H, 2.71; N, 6.28. Found: C, 43.05; H, 2.79; N, 6.25 %. MS (FAB): *m/e*, 892 (M^+).

4. NMR characterization

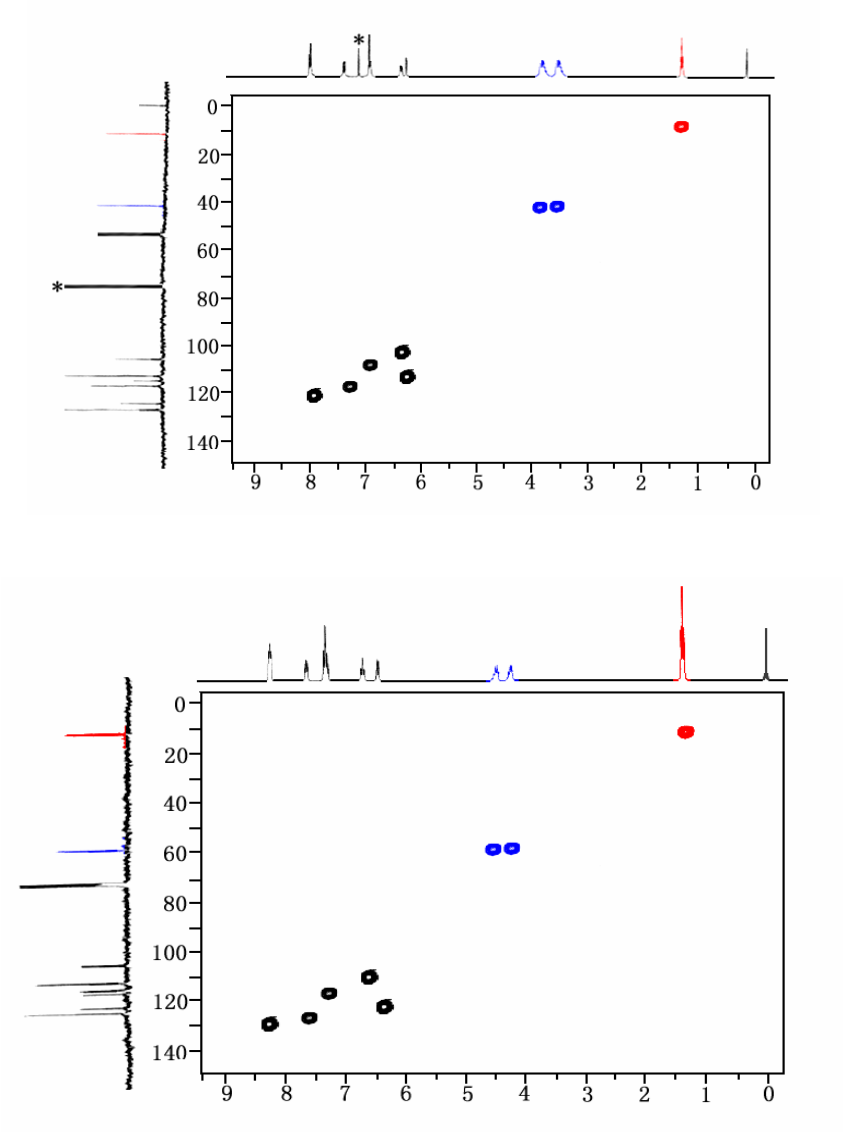

Fig. S1 ^{13}C-^{1}H COSY Spectra of **3** (up) and **4** (down) in $CDCl_3$

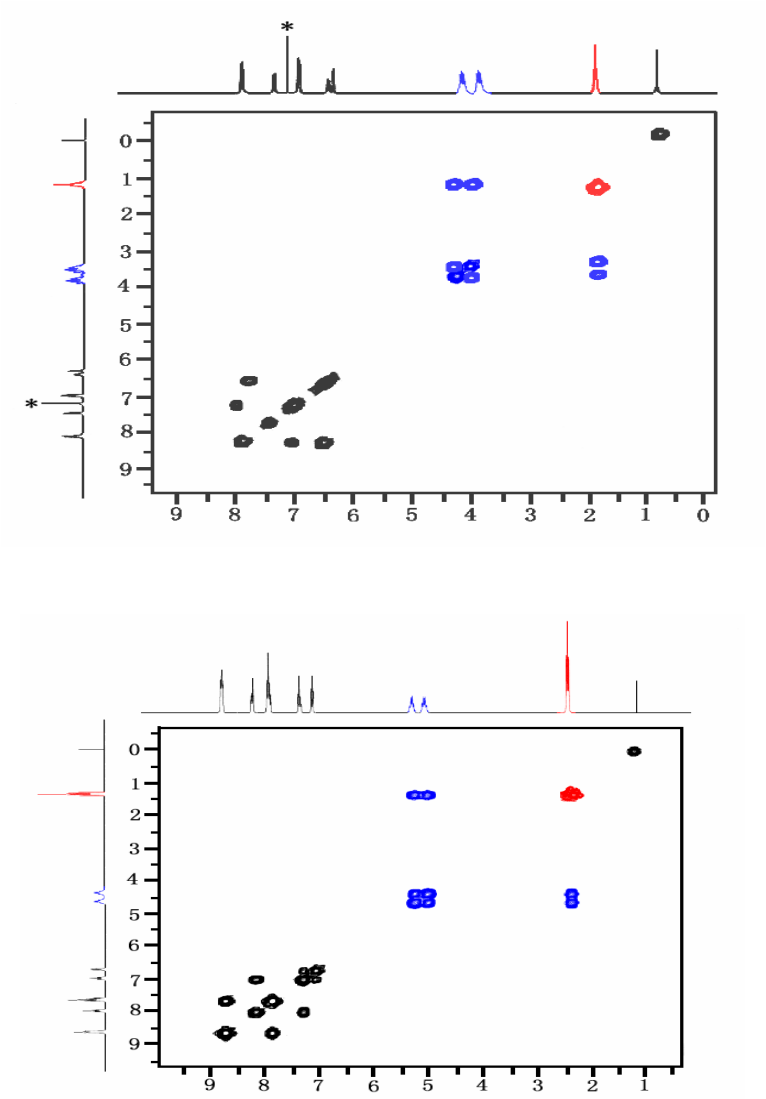

Fig. S2 ^{1}H-^{1}H COSY NMR Spectra of **3** (up) and **4** (down) in $CDCl_3$

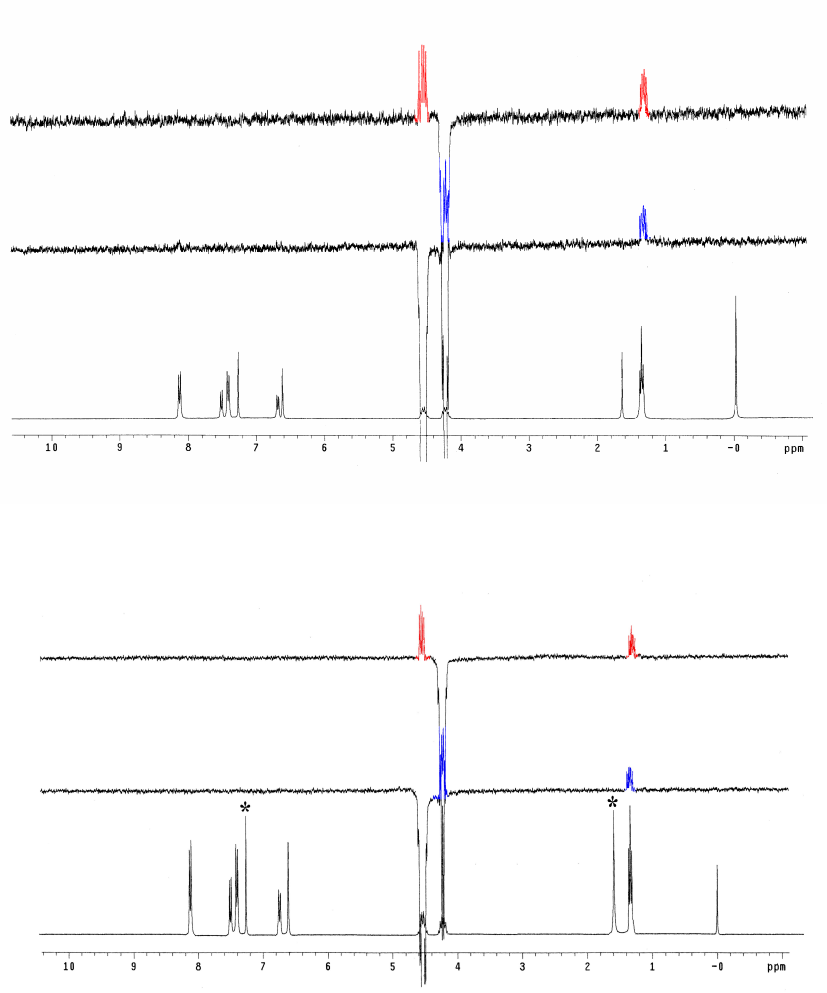

Fig. S3 One-dimensional NOE spectra of **3** (up) and **4** (down) in $CDCl_3$

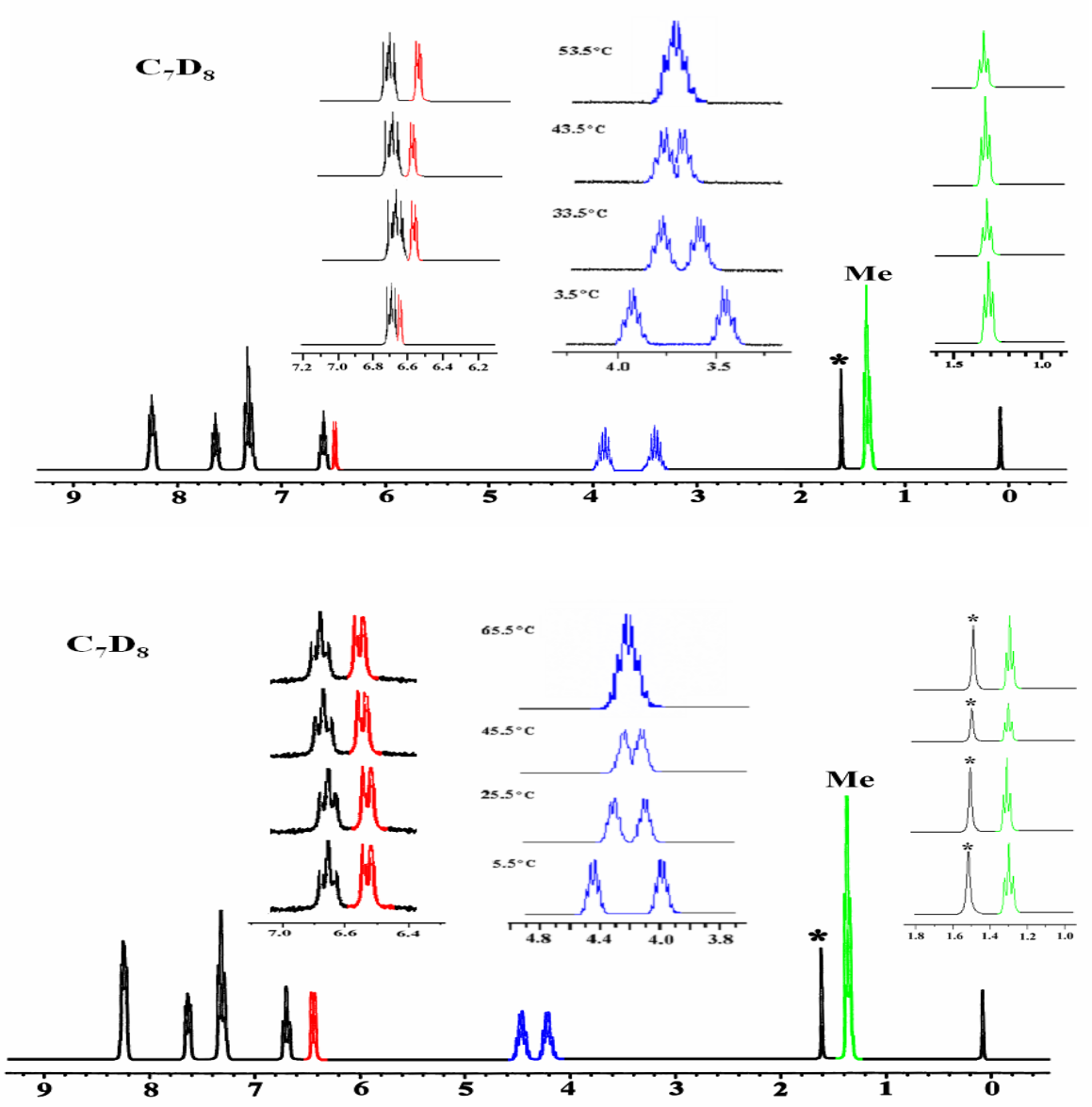

Fig. S4 Variable temperature ^{1}H NMR spectra of **3** (up) and **4** (down) in *d*-toluene, showing two group multiplets becoming closer, and merged at last.

5. Single crystal X-ray crystallography

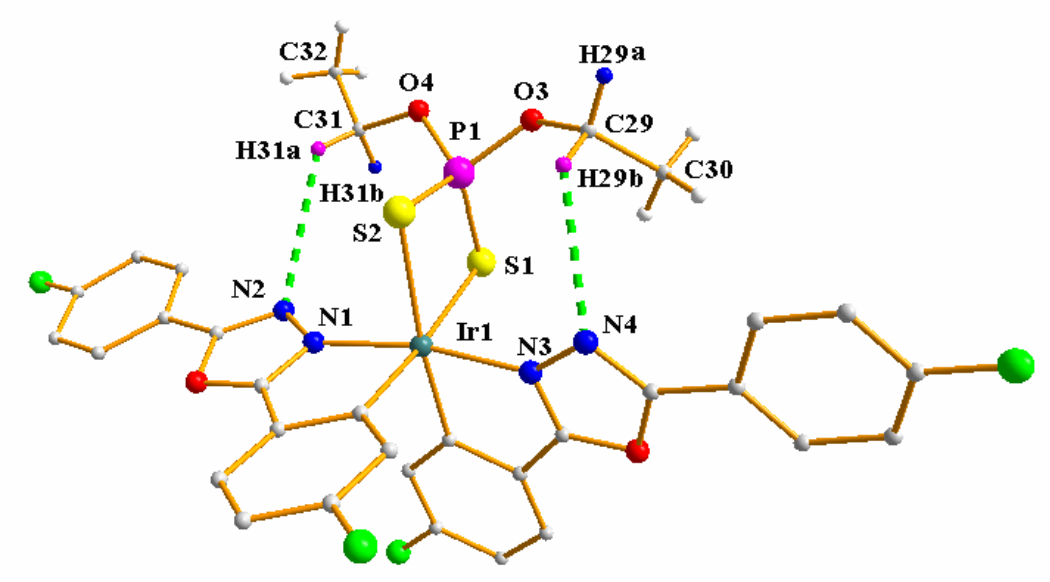

Fig. S5 Views of the molecular structure of **4**, showing van der Waals interactions between H atoms and N atoms.

Table S1 Crystal data and structure refinement for **4**

Crystal Data	**4**
Empirical formula	$C_{32}H_{24}O_4N_4F_4S_2PIr$
Formula weight	891.84
Crystal system	Triclinic
Space group	*P*-1
a	11.884(2) Å
b	12.611(3) Å
c	14.567(3) Å
α	77.01(3)°
β	66.69(3)°
γ	62.94(3)°
Volume	1783.0(6) $Å^3$
Z, Calculated density	2, 1.661 Mg/m^3
Absorption coefficient	3.968 mm^{-1}
Temperature	293(2) K
Wavelength (Mo-Ka)	0.71073 Å
Crystal size (mm)	0.10 x 0.08 x 0.06
Completeness (θ)	98.6 % (27.42 °)
Limiting indices	0≤h≤15, -14≤k≤16, -17≤l≤18
Reflections collected/unique	16756 / 8014 [R (int) = 0.042]
F(000)	872
Goodness-of-fit on F^2	1.088
Final R indices[I>2sigma (I)]	R1 = 0.0407, wR2 = 0.1120
R indices (F^2)	R1 = 0.0561, wR2 = 0.1212

Table S2 Selected bond lengths (Å) and angles (deg) for **4**

Bond lengths (Å)					
Ir(1)-C(18)	2.018(6)	Ir(1)-C(31)	2.039(6)	Ir(1)-N(1)	2.030(5)
Ir(1)-N(2)	2.043(5)	Ir(1)-S(1)	2.4770(17)	Ir(1)-S(2)	2.4885(17)
Bond angles (deg)					
C(18)-Ir(1)-C(31)	93.88(17)	C(18)-Ir(1)-N(1)	80.24(16)	C(31)-Ir(1)-N(1)	94.95(16)
N(1)-Ir(1)-N(2)	173.62(13)	C(18)-Ir(1)-O(1)	176.37(14)	O(1)-Ir(1)-O(2)	88.04(12)
N(2)-Ir(1)-O(2)	97.40(13)	N(1)-Ir(1)-O(2)	87.52(12)		

6. Electrochemical properties

Cyclic voltammetry (CV) were manipulated on CHI voltammetric analyzer at room temperature. Anhydrous CH_2Cl_2 and THF were used as the solvent under nitrogen atmosphere, respectively. Tetra(*n*-butyl)-ammoniumhexafluorophosphate ($TBAPF_6$) (0.1 M) was used as supporting electrolyte. The conventional three-electrode configuration consists of platinum working electrode, a platinum wire auxiliary electrode, and an Ag wire quasi-reference electrode. The redox potentials were calibrated versus a ferrocenium/ferrocene (Fc^+/Fc) redox couple used as an internal reference.

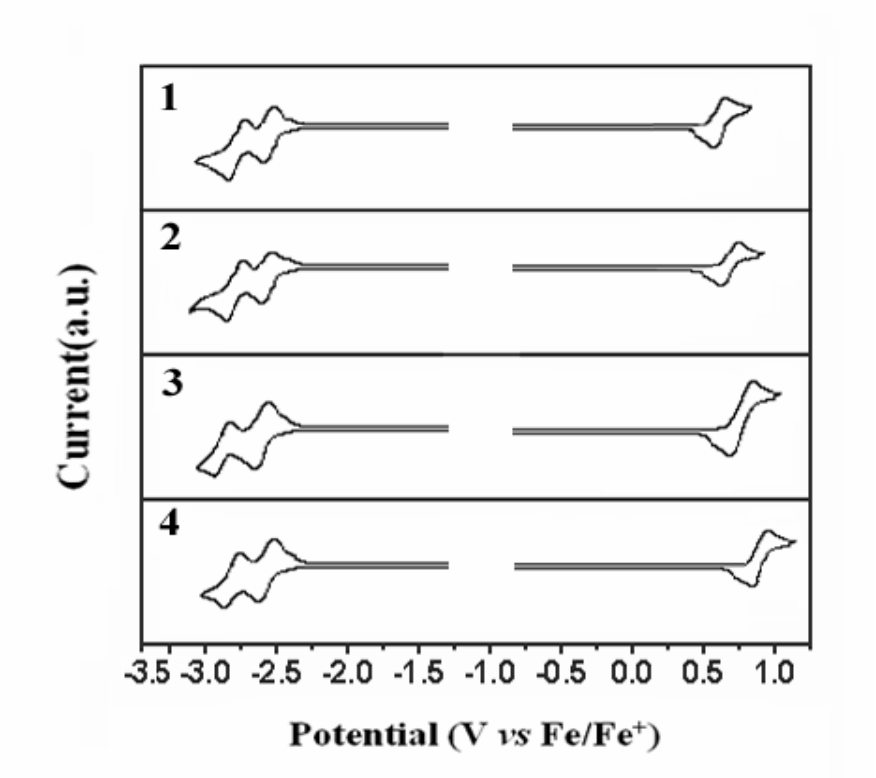

Fig. S6 Cyclic voltammograms of Ir (III) complexes

7. Photophysical properties

Table S3 Photophysical data for Ir (III) complexes.

Complex	UV-Vis λ_{abs} (log ε) nm		PL λ_{max} nm		Φ_f [c] (%)
	Solution[a]	Film[b]	Solution[a]	Film[b]	
1	246(3.9), 298(4.0), 355(3.2) 424(2.7), 465(2.0)	247, 263, 361 407, 467	500, 529	505, 535	35.2
2	230(3.8), 312(4.0), 369(3.3) 432(2.8), 468(2.1)	240, 275, 371 401, 472	479, 510	484, 516	43.5
3	238(3.8), 323(4.0), 402(3.3) 436(2.7), 472(2.0)	241, 326, 409 443, 474	470, 501	475, 507	32.3
4	241(3.9), 313(4.0), 397(3.2) 434(2.8), 469(2.2)	239, 324, 393 436, 471	466, 498	470, 503	9.6

[a] in CH_2Cl_2 solution at 298K. [b] in PMMA film (5 % weight ratio). [c] Quantum yield was measured in CH_2Cl_2 solution relative to quinine bisulfate (10^{-5} M in 1.0 N H_2SO_4).

8. Electroluminescence and Devices

Organic layers were fabricated by high-vacuum thermal evaporation onto a pre-cleaned indium tin oxide (ITO, 30Ω/square). The glass substrates were sequentially cleaned by detergent, deionized, water, ethanol, acetone and chloroform in ultrasonic bath and heated in an ultra-infrared dry oven. In a vacuum chamber with a pressure of < 10^{-4} Pa, 40 nm of (4,4'-bis{*N*-(1-naphthyl-*N*-phenyl-amino)biphenyl}) (NPB) as the hole transporting layer (HTL), 30 nm of Ir complexes doped 4,4'-biscarbazolybiphenyl (CBP) as the emitting layer, 10 nm of 2,9-dimethyl-4,7-diphenyl-1,10-phenanthroline (BCP) as a hole and exciton blocking layer, 30 nm of AlQ_3 as the electron transporting layer (ETL), and a cathode composed of 1 nm of lithium fluoride and 100 nm of aluminum were sequentially deposited onto the substrate to construct the device. The *J-V-B* of EL devices was measured at ambient condition with a Keithey 2400 Source meter and a Keithey 2000 Source multimeter equipped with a calibrated silicon photodiode. The EL spectra were measured by JY SPEX CCD3000 spectrometer.

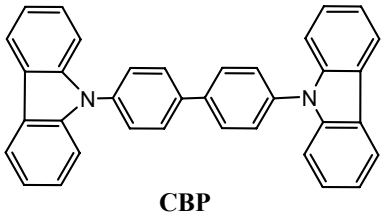

CBP

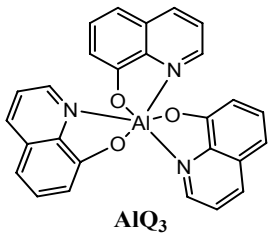

AlQ_3

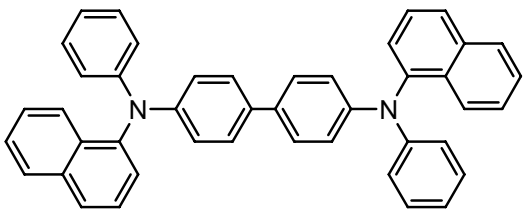

NPB

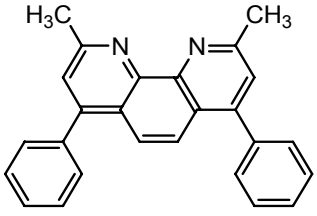

BCP

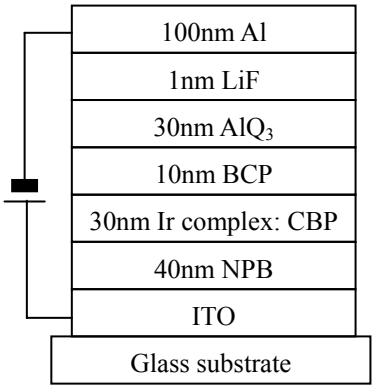

Fig. S7 The configuration of device and the molecular structures of the compounds used in the device.

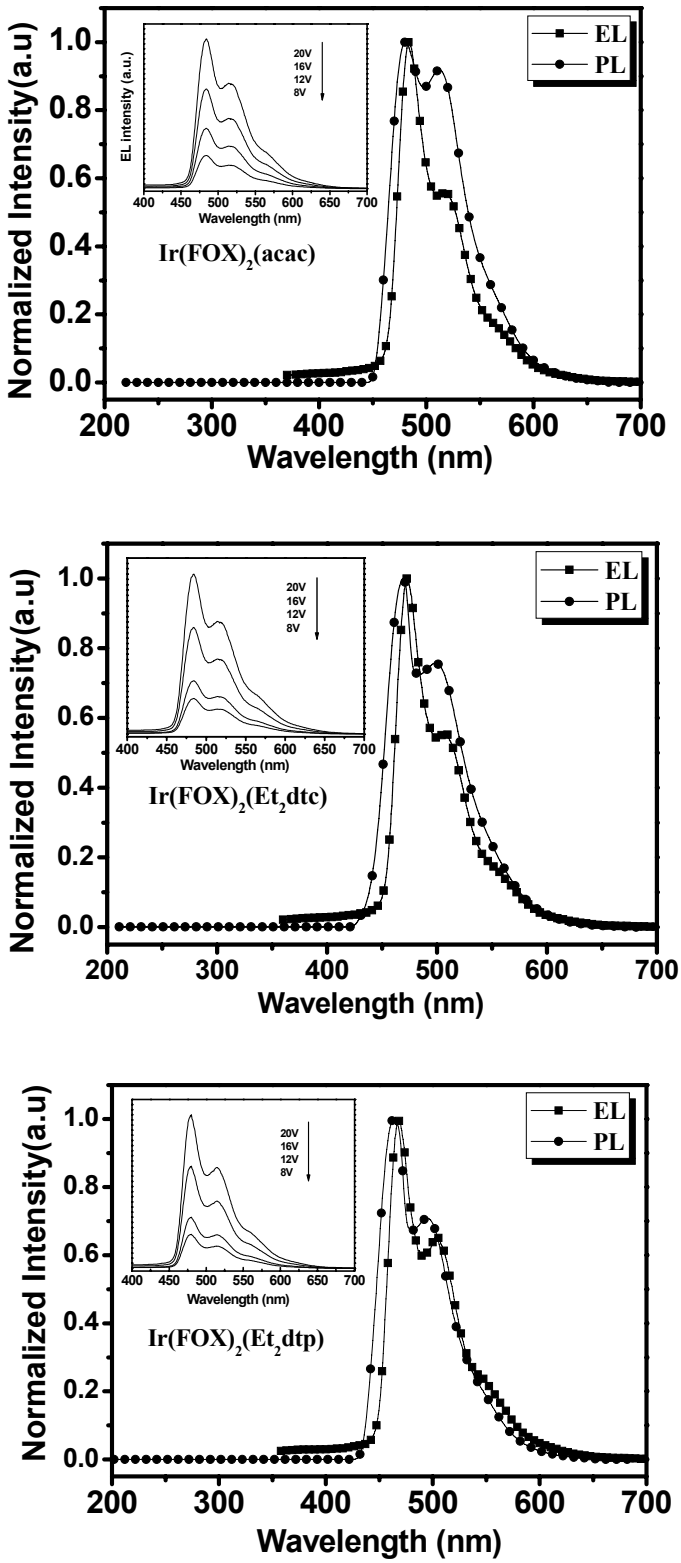

Fig. S8 EL spectra of devices at the driving voltage of 12 V using **2**(up), **3** (middle), **4**(down) as dopants, along with corresponding PL spectra in PMMA film for comparison. (Inset: EL spectra of devices dependent on the driving voltages).

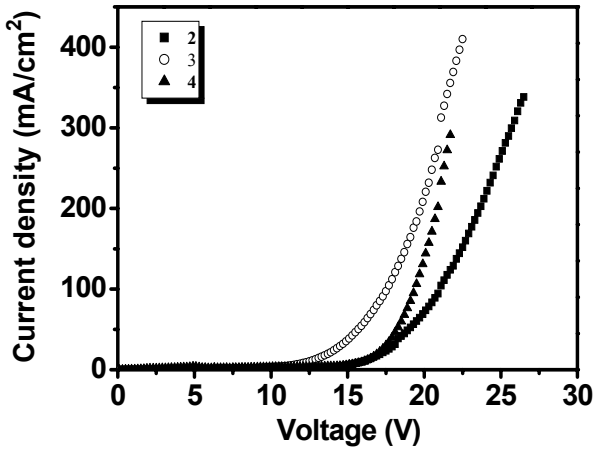

Fig. S9 Current density-voltage (*J-V*) curves of the devices using **2-4** as dopants at 5 % doping level

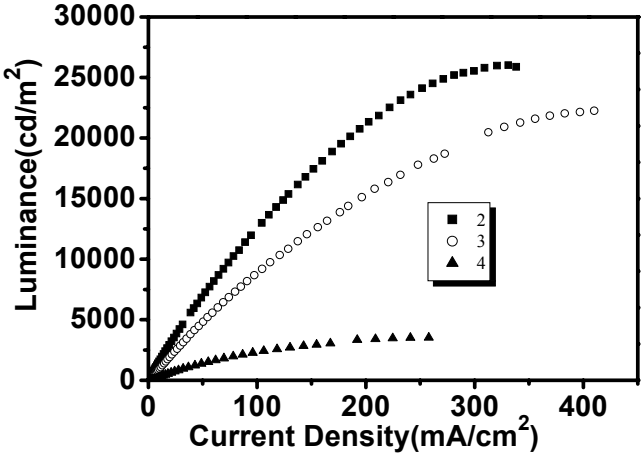

Fig. S10 Luminance-current density (*L-J*) curves of the devices using **2-4** as dopants at 5 % doping level

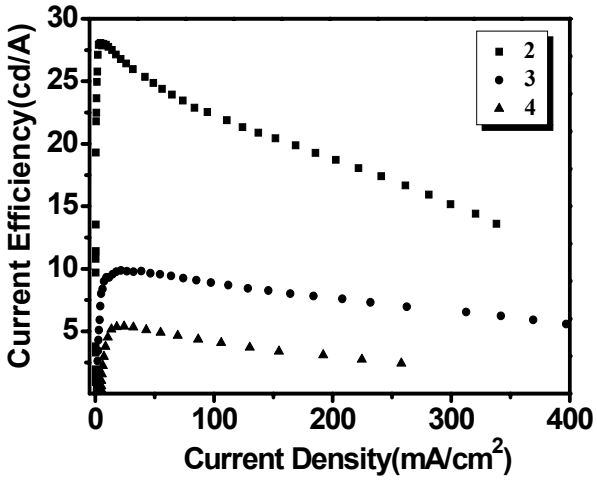

Fig. S11 Current efficiency-current density (η_c-*J*) curves of the devices using **2-4** as dopants at 5 % doping level

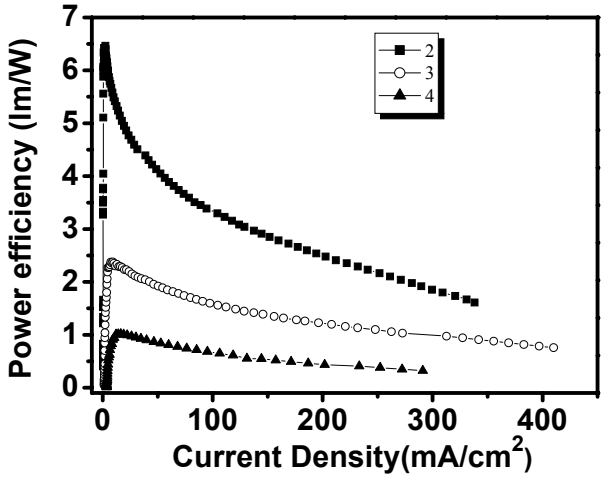

Fig. S12 Power efficiency-current density (η_p-J) curves of the devices using **2-4** as dopants at 5 % doping level.

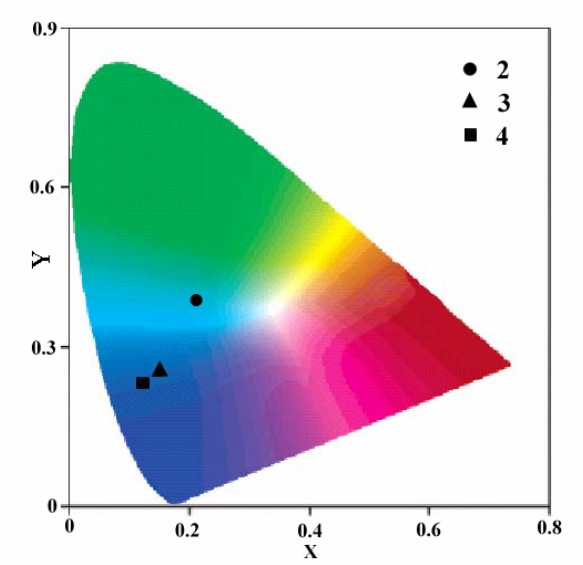

Fig. S13 CIE 1931 coordinates plot for the devices using **2-4** as dopants at 5 % doping level.

Table S4 EL performances of devices with the structure: ITO/NPB (40 nm)/CBP + Dopant (30 nm)/BCP (10 nm) /AlQ_3 (30 nm)/LiF(1 nm)/Al (100 nm).

Dopant phosphor	$Ir(FOX)_2(acac)$ (**2**)		$Ir(FOX)_2(Et_2dtc)$ (**5**)		$Ir(FOX)_2(Et_2dtp)$ (**9**)	
Wt %	3	5	3	5	3	5
L_{max} cd/m^2	17296	26015	18047	22250	2632	3659
Voltage V [a]	23.9	26.3	21.3	22.5	26.5	21.5
η_c cd/A [b]	18.50	26.95	7.72	9.75	3.65	5.40
η_c cd/A [c]	15.41	22.15	6.58	8.82	2.78	4.10
$\eta_{c\,max}$ cd/A	19.09	28.06	7.98	9.88	3.71	5.41
η_p lm/W [b]	3.80	4.93	1.80	2.23	0.53	0.45
η_p lm/W [c]	2.52	3.30	1.23	1.58	0.36	0.27
$\eta_{p\,max}$ lm/W	4.57	6.46	2.03	2.38	0.55	1.01
V_{ON} V[d]	4.7	4.9	4.7	5.5	4.5	4.8
CIE (X, Y)	(0.21, 0.35)	(0.22, 0.37)	(0.16, 0.27)	(0.16, 0.28)	(0.14, 0.25)	(0.14, 0.26)
El_{max} nm[e]	480	482	471	473	468	469

[a] Voltage at the maximum brightness. [b] Recorded at 20 mA/cm^2. [c] Recorded at 100 mA/cm^2. [d] Recorded at the brightness of 1 cd/m^2. [e] Recorded at the driving voltage of 12 V.